Features of Tuning Strategy for Field Oriented Control of PMSM Position Drive System with Two-mass Load

Dmitry V. Lukichev, Galina L. Demidova

***Abstract*—** This paper presents technique to tune the controllers for Field Oriented Control (FOC) of position servo drive system. Permanent magnet synchronous motor (PMSM) is used as a motor for this tracking system. Two algorithms of vector control (VC) are considered: Field Oriented Control (FOC) based on current model of motor and FOC based on voltage model of motor. Each algorithm determines the type of inverter and the structure of control scheme. In common motor and plant in this position tracking system are represented as two-mass load. Considered methods of tuning the controllers employ a simplified model of the motor and plant. Comparison of these FOC-algorithms is given in paper. A computer simulation shows the validity of the proposed algorithms.

***Keywords*—**permanent magnet synchronous motor, vector control, field oriented control, position tracking system, two-mass load, pulse-width modulated (PWM) inverter, Current-Regulated pulse-width modulated (CRPWM) inverter, magnitude optimum (MO), symmetric optimum (SO)

I. Introduction

DUE to their high efficiency and their simple design, permanent-magnet synchronous motors (PMSM) have been widely used in many industrial applications, particularly in the systems of precision movement and positioning of telescopes. These are two-mass systems that have low torsional resonance/anti-resonance frequencies because of low stiffness in the flexible shaft between a motor and load [1, 2]. So it is necessary to take into account when tuning the controllers in these systems.

In these systems PMSMs are often confronted with all kind of disturbances. These disturbances may arise by internal or external factors, for instance, friction force, working temperature and load disturbances.

Additionally, the dynamic model of a PMSM is highly nonlinear [3]. All of which makes it difficult to control.

There are some algorithms for control PMSM [4]. In classical control methods PI controllers are used in the position, speed and currents control loops [5]. Many variations and improvements have been made based on this control strategy. One way is the addition of the adaptation loop with a reference model to the basic system control loops [6]. Another method is intelligent control that uses Fuzzy controller [7] or Neural-Network controller [8]. However, these methods don't consider the cross-relation between the outer and inner control loops, which essentially limits its performance.

It is known that the PMSM Vector Control (VC) allows one to obtain a dynamical model similar to the DC machine. Vector control is a precise control method for both steady-state and transients. The first and most popular VC method is Field Oriented Control (FOC). This method is based on decoupling control of torque and flux [9, 10]. Therefore, this method allows for taking into account the nonlinear dynamics of the drive. Also, field-oriented control applies for high-performance motor applications, which can operate smoothly over the full speed range, can generate full torque at zero speed, and is capable of fast acceleration and deceleration.

The vector control system with a pulse-width modulated (PWM) inverter uses FOC based on voltage model of motor. The vector control system with a Current-Regulated pulse-width modulated (CRPWM) inverter uses FOC based on the current model of motor. So the type of inverter determines the structure of control scheme.

The aim of the paper is the methodology of controllers' tuning for both FOC-strategies and their application in tracking systems.

Research was conducted by mathematical modelling using an interactive environment for scientific and engineering calculations MATLAB/Simulink.

II. Mathematical model of PMSM

The mathematical model of the PMSM is [3] :

$$\begin{cases} \underline{u}_S = \underline{i}_S R_S + \dfrac{d\underline{\psi}_S}{dt}; \\ \underline{\psi}_S = L_S \underline{i}_S + \underline{\psi}_r; \\ T_e = \dfrac{3}{2} P \cdot \mathrm{mod}\left(\underline{\psi}_S \mathrm{x} \underline{i}_S\right) \end{cases} \quad (1)$$

The model (1) necessary to add to mechanical equation, which is defined as:

The Government of the Russian Federation, Grant 074-U01, financially supported this work.

D.V. Lukichev is with the ITMO UNIVERSITY, St. Petersburg, 197101 Russia, Electrical Engineering and Precision Electromechanical Systems Department (e-mail: lukichev@ets.ifmo.ru).

G.L. Demidova is with the Electrical Engineering and Precision Electromechanical Systems Department, ITMO UNIVERSITY, St. Petersburg, 197101 Russia (e-mail: demidova@ets.ifmo.ru).

$$J\frac{d\Omega}{dt} = T_e - T_l - B\Omega \qquad (2)$$

where J is the inertia of the motor and coupled load, T_l is the load torque, B is the friction coefficient and $\Omega = \omega / P$ is the mechanical angular speed, ω is the electrical angular speed.

The model of the PMSM in a stationary frame is discribed by following equations:

$$\begin{cases} u_{s\alpha} = R_s i_{s\alpha} + L_s \dfrac{di_{s\alpha}}{dt} - \Omega P \psi_r \sin\theta_e; \\ u_{s\beta} = R_s i_{s\beta} + L_s \dfrac{di_{s\beta}}{dt} + \Omega P \psi_r \cos\theta_e; \\ T_e = \dfrac{3}{2} P \psi_r \left(-i_{s\alpha} \sin\vartheta_e + i_{s\beta} \cos\theta_e \right) \end{cases} \qquad (3)$$

where $u_{s\alpha}$, $u_{s\beta}$, $i_{s\alpha}$ and $i_{s\beta}$ are respectively the motor voltages and currents in α-β coordinates. Regarding the motor parameters ψ_s, ψ_r are respectively the flux of stator and the flux of the permanent magnet, P is the number of pole pairs, R_s is the stator resistance and L_s is the stator inductance. T_e is the electromagnetic torque, $\theta_e = P \cdot \theta$, θ is angle of vector flux ψ_r and angle of rotor roration.

The model of PMSM in a stationary frame is shown in Fig.1.

The considered electric drive is constructed on the basis of a three-phase PMSM, controlled by transistors of the inverter using signals of position sensor. This optical encoder provides measurement of the angle of rotation and speed. The currents in motor windings are measured by current sensors.

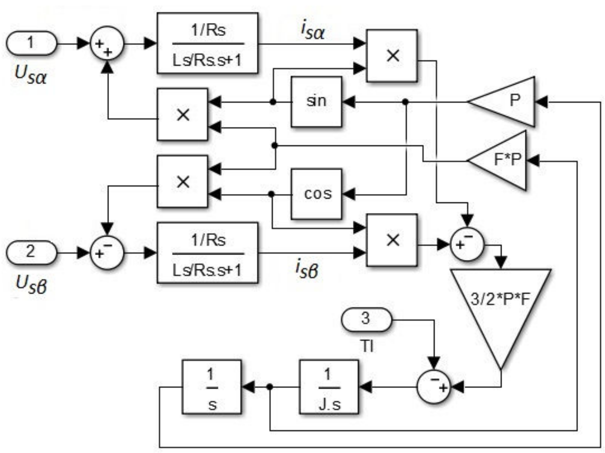

Fig.1. Model of PMSM in a stationary frame

Generalized structure of PMSM with load shown in Fig.2 is used to calculation controllers' coefficients.

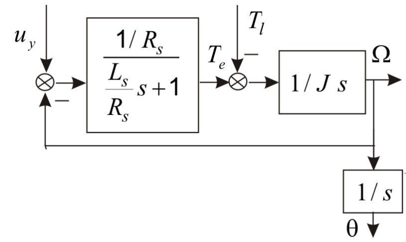

Fig.2. Generalized structure scheme of PMSM with load

III. Two-mass load

Analysis of the position drives, robots, and other high-performance drive leads to the conclusion that they can with sufficient accuracy be described by a model of a two-mass system with elastic coupling, and, if necessary, with the nonlinear friction and backlash. In our case, the kinematic scheme of the mechanical part of the drive system can be represented as shown in Fig. 1.

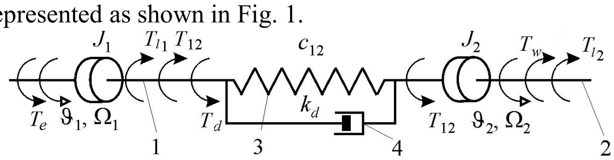

Fig.3. Kinematic scheme of the engine load, where 1 – the input side of the motor shaft driven by electromagnetic torque, 2 - the output side with controlled plant, 3 - torsion spring with stiffness coefficient c_{12} and damper 4.

Two-mass mechanical system comprises a lumped inertia of motor J_1 and a load J_2 coupled by a inertialess shaft with finite stiffness. The movement of both masses is described by angular speed Ω_1, Ω_2 and angles θ_1, θ_2, respective.

The drive system affect following torques (Fig.4.):

- load torque which is called "dry friction torque" $T_{l1} = T_{L1} \cdot sign(\Omega_1)$, $T_{l2} = T_{L2} \cdot sign(\Omega_2)$.
- torque of elastic coupling T_{12}
- wind load torque $T_w = f_w(t)$

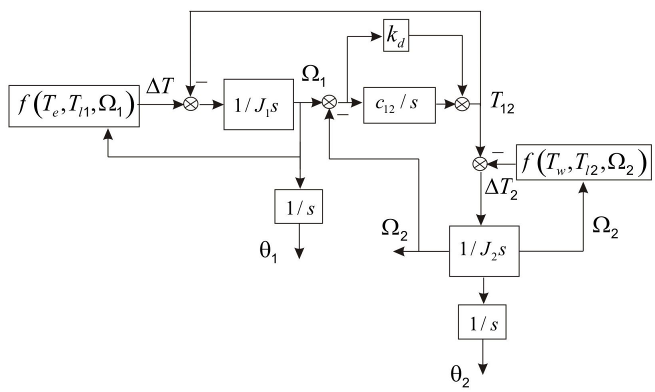

Fig.4. Block scheme of the two-mass load

Bode plot of transfer function $G_{\Omega 1}(s) = \frac{\Omega_1}{\Delta T}$ that describes two-mass load is presented in Fig.5.

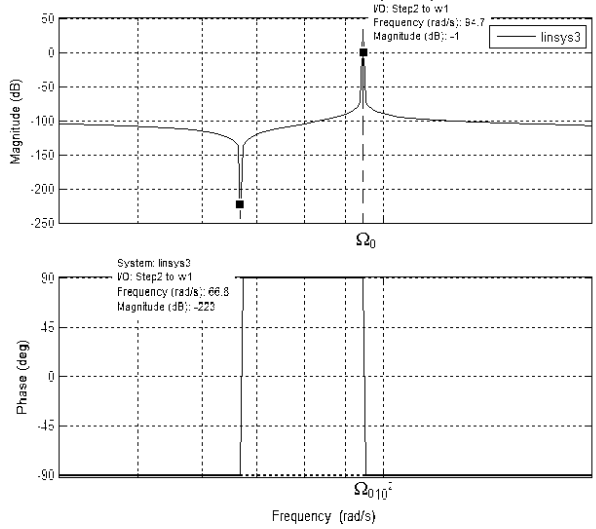

Fig.5. Bode Diagram for two-mass load

Bode plot clearly shows resonance frequencies related to poles and zeros of the transfer function $G_{\Omega 1}(s)$.

In particular $\Omega_0 = \sqrt{\frac{C_{12}(J_1 + J_2)}{J_1 J_2}}$ - mechanical resonance frequency of two-mass load. The existence of this frequency limits system response and must be taken into account when tuning the speed loop.

For calculation of controllers' coefficients, two-mass load is replaced to one-mass load as shown in Fig.2. Here $J = J_1 + J_2$.

IV. Field Oriented Control

The dynamic model of the PMSM presented in a rotating d-q frame fixed to the magnetic axis of the rotor is described by the following equations [3]:

$$\psi_{sd} = L_s i_{sd} + \Psi_r \tag{4}$$

$$\psi_{sq} = L_s i_{sq} \tag{5}$$

$$u_{sd} = R_s i_{sd} + L_s \frac{di_{sd}}{dt} - \omega L_s i_{sq} \tag{6}$$

$$u_{sq} = R_s i_{sq} + L_s \frac{di_{sq}}{dt} - \omega\left(L_s i_{sd} + \Psi_r\right) \tag{7}$$

$$T_e = \frac{3}{2} P\left(\psi_{sd} i_{sq} - \psi_{sq} i_{sd}\right) \tag{8}$$

where ψ_{sd}, ψ_{sq}, u_{sd}, u_{sq}, i_{sd} and i_{sq} are respectively the motor fluxes, voltages and currents in d-q coordinates.

In order to understand the torque production, (8) can be rewritten to obtain an expression of the torque as a function of the stator flux and the PM flux:

$$T_e = \frac{3}{2} P \frac{\Psi_s \Psi_r}{L_s} \sin\delta \tag{9}$$

It can be seen from (9) that the torque produced depends on the amplitude of the stator flux, the PM flux and the angle δ between both fluxes. It can also be concluded that maximum torque is produced when the angle between both fluxes is 90 degrees.

The principle of FOC is using rotating vectors (or phasors) in a complex coordinate system. Similarly to the IM, in the PMSM a decoupled control of the torque and flux magnitudes can be achieved, emulating a DC motor, by means of the FOC strategy. The magnitude and the phase of the controlled current are changed [10].

This is done using the d-q transformation that separates the components d and q of the stator current responsible for flux and torque production respectively. Due to the presence of the constant flux of the permanent magnet, there is no need to generate flux by means of the i_{sd} current, and this current can be kept to a zero value i_{sd} =0, which in turns decreases the stator current and increases the efficiency of the drive [11].

Fig. 6 describes the equations (6), (7) in the form of a vector diagram.

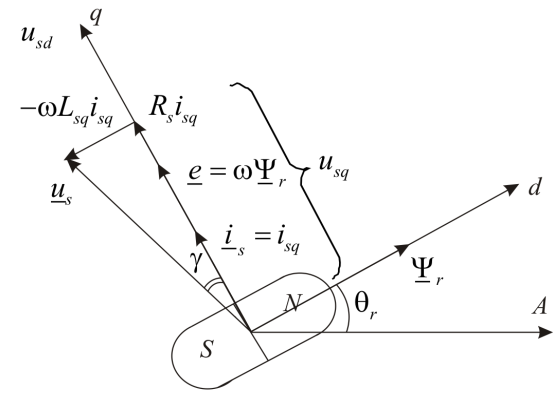

Fig.6. Vector diagram in rotating d-q frame

The fact that the torque can be controlled by means of i_{sq} comes from the following simplification of (4),(8), valid for Surface Mounted (SM) PMSM:

$$T_e = \frac{3}{2} P \Psi_r i_{sq} = C_T \Psi_r i_{sq} \tag{10}$$

where $C_T = 3P/2$

V. Magnitude Optimum (MO) and Symmetric Optimum (SO) Tuning Methods for PID Controllers

In order to receive a reasonable control performance it is necessary to control the parameters of the PI controllers included in the FOC scheme. It is well known two methods of parametric optimization: the MO and SO criterions. These two methods employ an approximate transfer function of the system to be controlled. Several parameter identification and mathematical modelling of the system are consequently needed. The MO method expects the system's transfer function in open loop of the following form:

$$G(s) = \frac{1}{2T_\mu s(1+T_\mu s)} \tag{11}$$

The SO method assumes the system's open loop transfer function as follows:

$$G(s) = \frac{4T_\mu s+1}{8T_\mu s(1+T_\mu s)} \tag{12}$$

The transfer functions system for the MO and SO in closed loop are present in evaluates (13)-(14) respectively:

$$G(s) = \frac{1}{2T_\mu^{\,2} s^2 + 2T_\mu s + 1} \approx \frac{1}{2T_\mu s+1} \tag{13}$$

$$G(s) = \frac{4T_\mu s+1}{8T_\mu^{\,3} s^3 + 8T_\mu^{\,2} s^2 + 4T_\mu s + 1} \tag{14}$$

where T_μ is sum of all small delays in loop. Also T_μ needs to be much smaller than the time constant of the system. The step response of both transfer functions in closed loop including the PI controller designed using the MO and SO criterions is as shown in Fig. 7. Table I presents the main features of the step responses obtained with both methods.

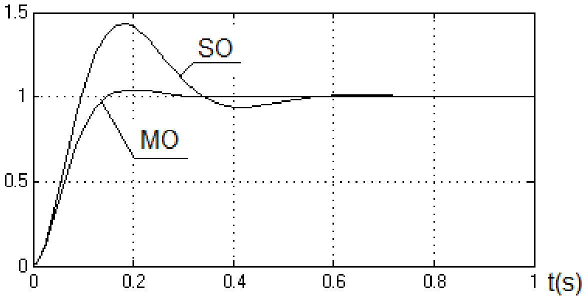

Fig. 7. MO and SO characteristic step responses

Tab. I. Step responses for MO and SO methods

Optimum / Parameter	MO	SO
Rise time	$4.7T_\mu$	$3.1T_\mu$
Settling time (2%)	$8.4T_\mu$	$16.5T_\mu$
Overshoot	4.3%	43.4%
Phase Margin	65.5°	37°

If both methods are compared it can be said that the SO is faster regarding disturbance rejection, which makes it suitable for external control loops. On the other hand MO has a smaller settling time and lower overshoot, which makes it appropriate to have quicker and more accurate inner loops.

VI. Field Oriented Control Based on Voltage Model of Motor

The control scheme of the FOC strategy based on voltage model of motor (6)-(7),(10) is shown in Fig. 8

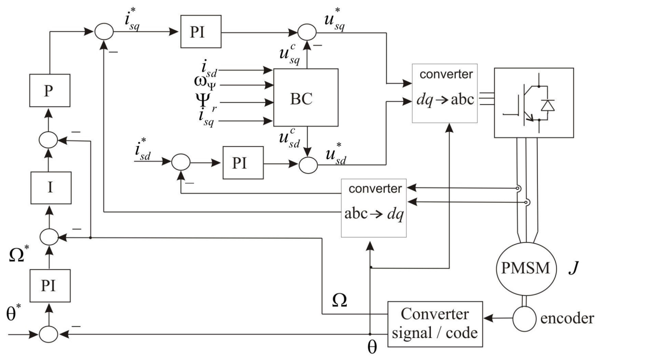

Fig. 8. The control scheme of the FOC strategy in the system with PWM inverter

For control of position servo drive system, it is proposed to use a four-loop cascade control structure with a position loop, speed loops and currents loop.

Block *abc→dq* is used to transform real currents of windings i_α, i_b, i_c to i_{sd} i_{sq} , which are *dc* quantities in the synchronous rotating frame:

$$\begin{aligned} i_{sd} &= \frac{2}{\sqrt{3}}[i_{sa}\sin(\theta_e + \frac{\pi}{3}) + i_{sb}\sin\theta_e] \\ i_{sq} &= \frac{2}{\sqrt{3}}[i_{sa}\cos(\theta_e + \frac{\pi}{3}) + i_{sb}\cos\vartheta_e] \end{aligned} \tag{15}$$

Block *dq→abc* performs the inverse transformation.

The compensation block of cross-relation (BC) provides the following signals:

$$\begin{aligned} u^c_{sd} &= -\frac{1}{K_{INV}}\omega L_s i_{sq} \\ u^c_{sq} &= \frac{1}{K_{INV}}\omega\left(L_s i_{sd} + \Psi_r\right) \end{aligned} \tag{16}$$

A. Current loop (i_{sd} control)

Fig. 9 shows the block diagram of the current control in closed loop.

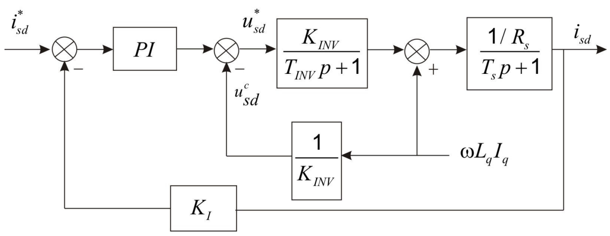

Fig. 9. Current loop block diagram

Current loop is tuned with help *PI* controller on magnitude optimum with the time constant $T_{\mu\_id} = T_{INV}$ related with the delay of inverter according to the expressions:

$$\begin{aligned} K_{P\_id} &= L_s / 2K_{INV}K_I T_{INV} \\ K_{I\_id} &= R_s / 2K_{INV}K_I T_{INV} \end{aligned} \tag{17}$$

where K_{inv} - amplification factor of the inverter, K_I -

feedback coefficient.

So system's close loop transfer function:

$$G_{id}(s)=\frac{1/K_I}{2T_{INV}^2 s^2+2T_{INV} s+1}\approx\frac{1/K_I}{2T_{INV} s+1} \quad (18)$$

B. Current loop (i_{sq} control)

In order to tune the *PI* current controller in *q* axis, it can be followed the same procedure described, but in this case using compensation signal $u_{sq}^c=\frac{1}{K_{INV}}\omega\left(L_s i_{sd}+\Psi_r\right)$. So i_{sq} current loop is tuned with help from the *PI* controller on magnitude optimum with the same values for K_{P_iq}, K_{I_iq} (see Equation 17).

C. Internal and external speed

Taking into account the Expression 10 and transfer function of inner current loop (18), one can obtain a block diagram of speed loops that is shown in Fig. 10

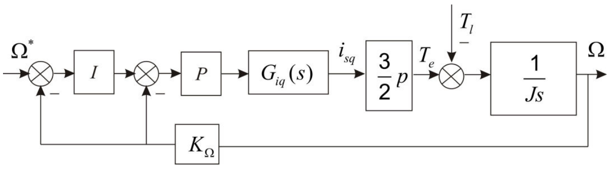

Fig. 10. Speed loops block diagram

Inner speed loop is tuned with help *P* controller on exponential process with the time constant $T_{\mu\_s}>2T_{INV}$.

$$K_{P\_s}=(J_1+J_2)K_I/(C_T\cdot T_{\mu\_s}K_\Omega) \quad (19)$$

where $T_{\mu\_s}=1/(2\Omega_{0r})$ is determined from the implementation of the bandwidth $\Omega_{0r}<\Omega_0/\sqrt[4]{\gamma^3}$, $\gamma=(J_1+J_2)/J_1$.

The magnitude optimization method is used for tuning external speed loop using *I* controller with coefficient:

$$K_{I\_s}=1/(2T_{\mu\_s}) \quad (20)$$

D. Position loop

Symmetric optimization method is used for position loop of control scheme with the *PI*-controller. Coefficients of *PI* position controller are determined as:

$$\begin{aligned}K_{P\_\theta}&=K_\Omega/(4T_{\mu\_s}K_\theta)\\ K_{I\_\theta}&=K_{P\_\theta}/(8T_{\mu\_s})\end{aligned}. \quad (21)$$

The transfer function of the closed loop position control in accordance with the configured controllers is:

$$W_\vartheta=\frac{\vartheta}{\vartheta^*}=\frac{(4T_\mu+1)}{(8T_\mu^3 s^3+8T_\mu^2 s^2+4T_\mu s+1)K_\theta} \quad (22)$$

where $T_\mu=2T_{\mu\_s}$.

The result of simulation of four-loop FOC system of PMSM based on voltage model of motor is shown in Fig.14.

VII. Field Oriented Control Based on Current Model of Motor

The structure of the FOC strategy based on current model of motor (10) is shown in Fig. 11. This FOC strategy is realized with help Current-Regulated pulse-width modulated (CRPWM) inverter.

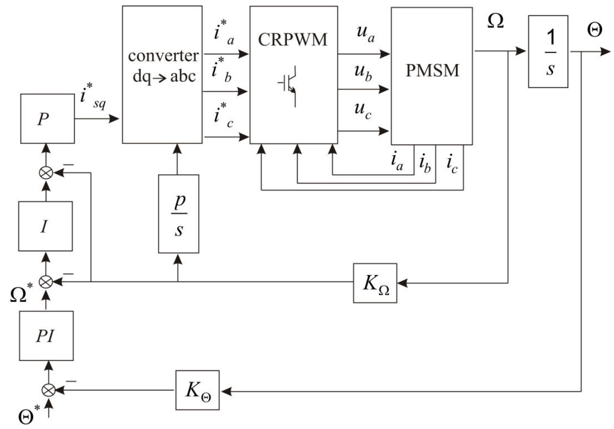

Fig.11. FOC with Current-Regulated pulse-width modulated (CRPWM) inverter

The principle of operation of the CRPWM inverter and transient process in it are shown in Fig.12 [11, 12].

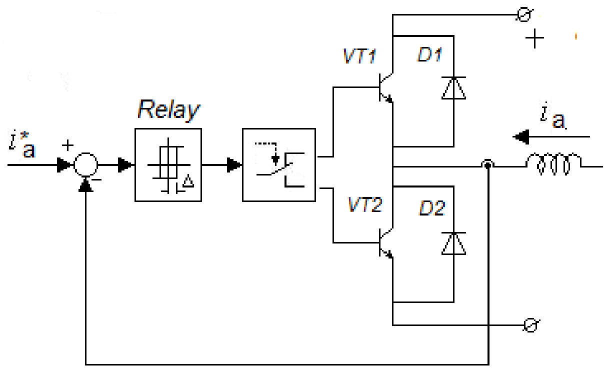

Fig.12a. The principle of operation of the CRPWM inverter

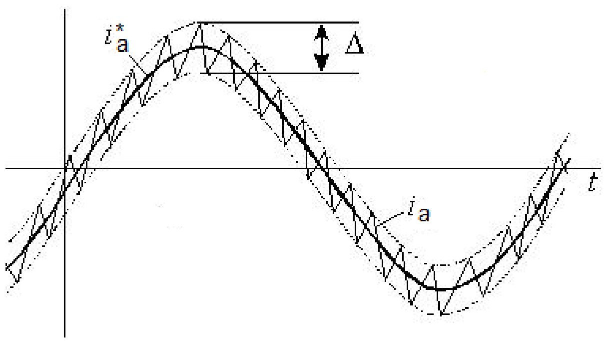

Fig.12b. Transient process in the CRPWM inverter

If the CRPWM inverter is ideal or has sufficiently large switching frequency that $i_a = i_a^*,\ i_b = i_b^*,\ i_c = i_c^*$ and the structure shown in Fig. 11 is transformed to the structure in Fig. 13. In this Figure PMSM is presented by current model of motor which is a part of voltage model of motor in *d-q* coordinates with condition i_{sd} =0.

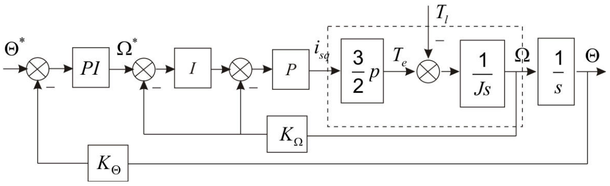

Fig.13. Equivalent structural scheme FOC with CRPWM inverter

Coefficients of *PI* position controller and *P* and *I* speed controllers are determined based on the structure of Figure 13 according to the expressions:

- internal speed loop with *P* controller (exponential process with the smaller time constant T_{μ_s}):

$$K_{P1\_s} = 2J/(3P\Psi_r K_\Omega T_{\mu\_s}) \tag{23}$$

-external speed loop with *I* controller (magnitude optimum):

$$K_{I1\_s} = 1/(2T_{\mu\_s}) \tag{24}$$

-position loop with *PI* controller (symmetric optimum):

$$K_{P1\_\theta} = K_\Omega / (4T_{\mu\_s} K_\theta)$$
$$K_{I1\_\theta} = K_{P1\_\theta} / (8T_{\mu\_s}) \tag{25}$$

The transfer function of the closed loop position control is the same as $W_\vartheta(s)$ in expression (22).

VIII. Simulation Experiments

This section shows the results regarding the tuning controllers in presented FOC algorithms. Simulation experiments have been carried out using interactive environment for scientific and engineering calculations *MATLAB*/*Simulink*.

The parameters of the PMSM are given in Tab.II. The simulation results are shown in Fig. 14-15.

Table II. Parameters of motor and load

Output Power (P_n)	5265W
Supply voltage (U)	540 V
Number of pole pairs (P)	48
Nominal Torque (T_n)	345 N·m
Nominal Current (I_n)	11,3 A
Stator resistance (R_s)	2.6 Ohm
Stator inductance (L_s)	26.2 mH
Permanent Magnet Flux (ψ_r)	0,52 Wb
The inertia of motor (J_1)	5,31 kg·m^2
The inertia of plant (J_2)	1596 kg·m^2
Stiffness coeff. c_{12}	3,9·10^7 N·m/rad
Load torque (T_l)	100 N·m

Fig. 14. shows the closed-loop response in FOC PMSM system to the step reference signal and step load torque. The processes in the FOC with PWM inverter and in the FOC with CRPWM inverter have have close value of response. Overshoot can be reduced by using a filter with transfer function $G_{filter}(s) = \dfrac{1}{4T_\mu s + 1}$.

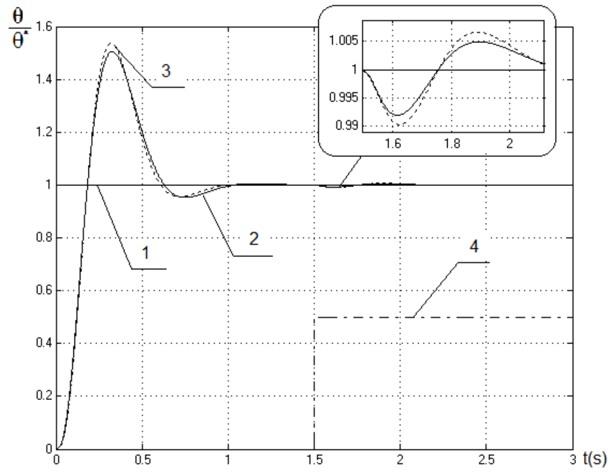

Fig.14. Transient processes in the FOC system with CRPWM inverter 2 and in the FOC system with PWM inverter 3, 1 - reference position signal, 4- load torque

Fig. 15 gives the result of the position regulation which illustrates tuned controllers can provide good control to realize the tracking to desired angle position in two-mass system.

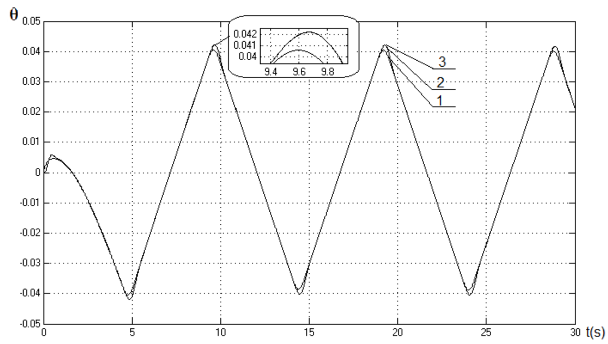

Fig.15. Tracking mode in the two-mass FOC systems, where 1 – reference position signal, 2 – position signal in FOC system with current-regulated-PWM inverter, 3 - position signal in FOC system with PWM inverter

IX. Conclusion

The paper presents a description and comparison two vector control strategies for PMSM drives: FOC in the system with current-regulated-PWM inverter and FOC in the system with PWM inverter and their use in the tracking servo drive system. A step by step method of controllers' tuning is given. In position tracking PMSM servo drive system position loop and two speed loops are used. Internal speed loop is tuned to provide the bandwidth $\Omega_{0r} < \Omega_0 / \sqrt[4]{\gamma^3}$ related with mechanical resonance frequency of two-mass load.

The simulation results have been given based on the tuned controllers that show the good position regulation performance on tracking the desired position of PMSM.

REFERENCES

[1] C. Beards, Vibration analysis and control systemdynamics, Halsted Press, 1981.

[2] Yu.A. Bortsov, G.G. Sokolovskiy, Automatic Electric with elastic ties, Saint-Petersburg, Energoatomizdat, 1992.

[3] R. Krishnan, Electronic Motor Drives: Modeling, Analysis and Control, Upper Saddle River, New Jersey, USA: Prentice Hall, Feb. 2001.

[4] Z. Yaou, Z. Wansheng, K. Xiaomig. Control of the Permanent Magnet Synchronous Motor Using Model Reference Dynamic Inversion, *WSEAS Transactions on Systems and Control*, issue 5, vol.5, 2010, pp.301-311

[5] V.A. Tolmachev, Synthesis of the electric servo axes of positioned, *Scientific and Technical Journal «Priborostroenie»*, vol. 51, no. 6, 2008, pp. 68-72.

[6] G.L. Demidova, S.Yu Lovlin, M.Kh. Tsvetkova, Synthesis of Follow-up Electric Drive of telescope's azimuth axis with reference model in position contour, *Vestnik IGEU*, no. 2, 2011, pp. 77–81.

[7] G.L.Demidova, D.V.Lukichev, Fuzzy Control of the Position Servo Motor Drives with Elasticity and Friction, *Proceedings of the 18th International Conference on Systems (part of CSCC '14)* vol.1 pp. 157-160

[8] Fayez F.M. El-Sousy. An Adaptive Neural-Network Model-Following Speed Control of PMSM Drives for Electric Vehicle Application, *Proceedings of the 9th WSEAS International Conference on Applied Mathematics*, 2006, pp.412-417

[9] Blaschke F., The principle of field-orientation as applied to the transvector closed-loop control system for rotating-field machines, Siemens Rev., vol 34, pp. 217-220, 1972.

[10] Bayer K.-H., Waldmann H., Weibezahl M. Die TRANSVEKTOR-Regelung für den feldorientierten Betrieb einer Synchronmaschine, Siemens-Zeitschrift, 45 (1971), S. 765–768.

[11] A. K. Daud, B. Alsayid, A. Zaidan. DSP Based Simulator for Field Oriented Control of the Surface Permanent Magnet Synchronous Motor Drive, *International Journal Of Circuits, Systems And Signal Processing*, issue 1,vol.6, 2012, pp.29-37

[12] B. Bossoufi, M. Karim, S. IONIТĂ, A. Larioui, G.V. Iana. Matlab & Simulink Simulation with FPGA-Based Implementation Sliding Mode Control of a Permanent Magnet Synchronous Machine Drive, *WSEAS Transactions on Systems and Control*, issue 3, vol.6, 2011, pp.92-103